# Observing the growth of individual actin filaments in cell extracts by time-lapse atomic force microscopy

Tiina Lehto[a,b], Marta Miaczynska[b], Marino Zerial[b], Daniel J. Müller[a,b,*], Fedor Severin[b,**]

[a] *BIOTEC, Technical University Dresden, 01609 Dresden, Germany*
[b] *Max Planck Institute of Molecular Cell Biology and Genetics, Pfotenhauerstrasse 108, D-01307 Dresden, Germany*

Received 30 June 2003; accepted 13 July 2003

First published online 14 August 2003

Edited by Amy McGough

**Abstract High-resolution atomic force microscopy (AFM) was applied to directly observe the dynamic assembly of single actin filaments in HeLa cell extracts in vitro. The F-actin filaments established a dynamic network and formed different types of junctions and branches. The connections of this network were X-, Y- or T-shaped. It was found that the actin filaments were densely covered by endosomes and vesicles from the cell extract, which are thought to stabilize their structures. Using time-lapse AFM, the growth, shrinkage, branching and the interaction of actin filaments with endosomes could be characterized. Our results indicate that the majority of F-actin filaments are static in HeLa extract and that only a minor fraction of filaments undergo dynamic changes. Furthermore, the AFM imaging approach not only provides unique insights into the assembly and dynamics of actin networks; it also builds an avenue to study in vitro assays of complex biological systems.**


*Key words:* Actin; Atomic force microscopy; Branching; Cell extract; Endosome

## 1. Introduction

Fluorescence microscopy, frequently used in modern biological research, requires labeling the molecules of particular interest with fluorophores. These chemically fixed labels have the potential to influence the native behavior of the labeled molecule [1,2]. Chemical reactions limit the lifetime of the fluorophore and thereby the visualization process. Most importantly however, molecules other than the labeled ones will not be visualized by optical methods. To overcome this limitation multicolor imaging by the use of various fluorophores allows simultaneous imaging of different biological structures. However, the number of colors that are simultaneously detectable is presently limited to a few and the selection of structures that may be observed has to be done carefully.

Actin in cells polymerizes into filaments (F-actin). In nonmuscle cells F-actin is organized mostly in bundles (stress fibers) and the diffuse network close to the cell cortex. The dynamic growth behavior of F-actin provides the basis for cell locomotion, cytokinesis and certain types of organelle motility inside the cell (see [3] for review). So far imaging of individual actin filament dynamics in vitro has been performed using light microscopy [4]. In contrast to optical microscopy, the exceptionally high signal-to-noise ratio of the atomic force microscope (AFM [5]) allows the observation of single unlabeled macromolecules in a heterogeneous environment [6]. AFM imaging of biological samples is performed in buffer solution and at ambient temperatures [7], which allows the imaging of living cells [8] and single proteins at work [9,10]. Such experiments can be performed over a time range of several hours without destruction of individual proteins or disturbing their inherent assembly. We report here an approach to study the dynamics of individual actin filaments in the cytosol by AFM. The presented method allows visualizing the growth/shrinkage of individual filaments in physiologically relevant buffer solution, their formation of networks and their association with membrane organelles.

## 2. Materials and methods

### 2.1. Sample preparation

HeLa cytosol and endosomes were prepared as described in [11]

First, 20 μl of endosomes were adsorbed to the support for 5 min. Then the liquid was aspirated and 50 μl of HeLa cytosol was added. To verify that the observed filaments were F-actin we tried to inhibit the filament growth by 5 μg/ml cytochalasin D. Alternatively, we omitted ATP from the reaction. In both cases, no filaments were detected, indicating that the observed filaments were polymerized from actin.

### 2.2. AFM

The AFM (Nanoscope III, Digital Instruments, Santa Barbara, CA, USA) was operated in buffer solution using the standard fluid cell, without an O-ring. Imaging was performed in tapping mode. The oxide-sharpened $Si_3N_4$ cantilevers (OMCL TR400PS, Olympus, Tokyo, Japan) employed had a nominal force constant of 0.09 N/m and a resonance frequency close to 9 kHz in water. The microscope was operated at conditions (tapping frequency close to resonance and amplitude) which allowed high precision control of the imaging process and the applied force to be $\leq 100$ pN [12]. All samples were imaged and manipulated in buffer solution at 21°C.

## 3. Results and discussion

### 3.1. Observing the polymerization of individual actin filaments

Within the past decade AFM has become an established method to image biological objects under native conditions at (sub-)nanometer resolution. In many AFM preparations free particles and proteins resulting from the buffer solution easily contaminate the AFM tip [13], thereby significantly

*Corresponding author. Fax: (49)-351-210 2020.
**Corresponding author. Fax: (49)-351-210 2020.
*E-mail addresses:* mueller@mpi-cbg.de (D.J. Müller), severin@mpi-cbg.de (F. Severin).

*Abbreviations:* AFM, atomic force microscopy

0014-5793/03/$22.00 
doi:10.1016/S0014-5793(03)00867-6

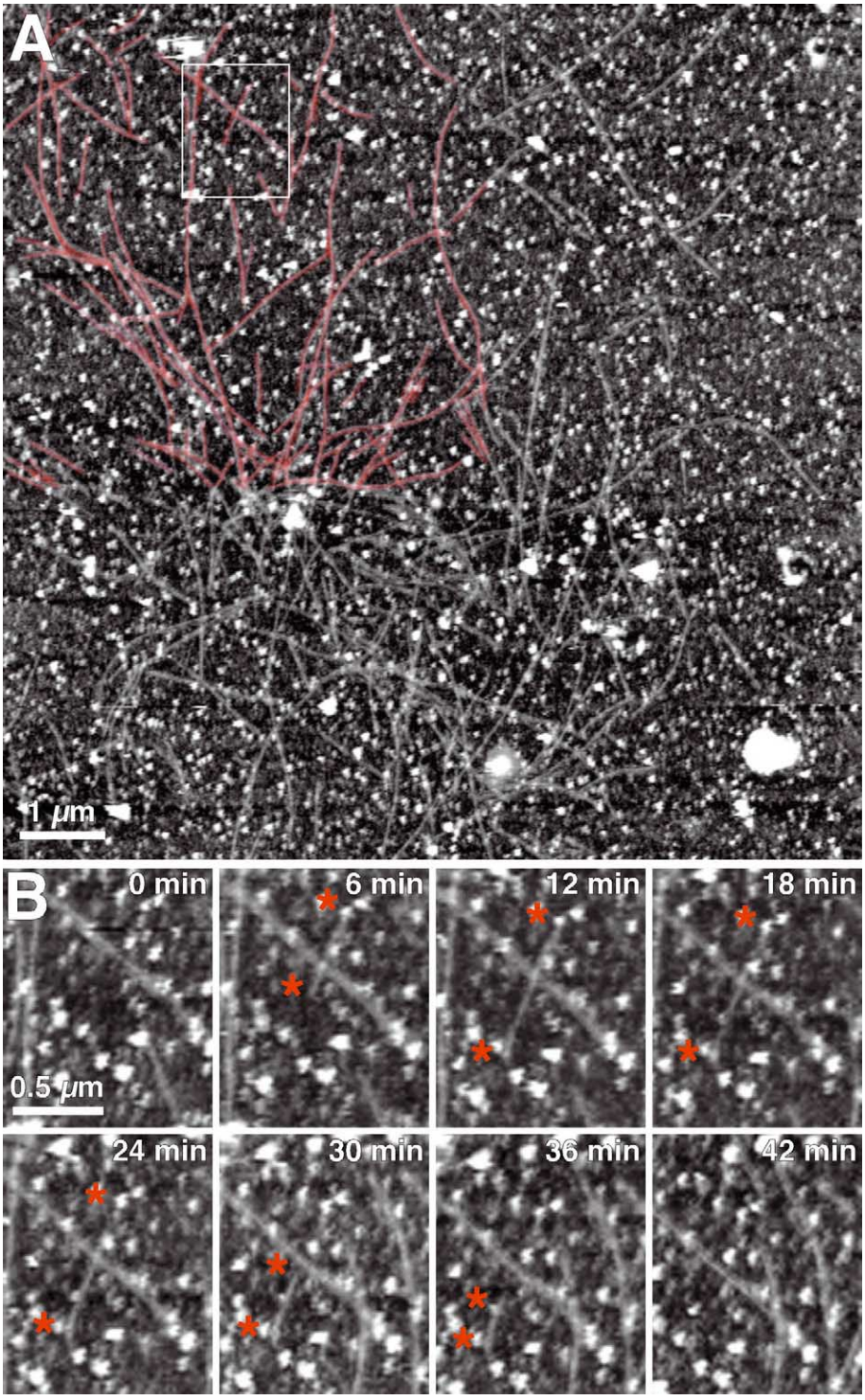


Fig. 1. Observing actin growth by time-lapse AFM. A: Shortly after the injection of HeLa cytosol individual actin filaments were observed on the supporting mica surface. The support was heavily decorated with endosomes and the macromolecules resulting from the cytosol. In the top left part of the image the filaments are highlighted in red. B: Dynamics of an individual actin filament. 0 min, enlarged region of A. After a time of 6 min the same surface area was imaged and showed an actin filament being polymerized. Asterisks mark the filament ends. One end of the filament is continuously growing (12 and 24 min). Suddenly, the polymerization of the lower end stops while the other filamentous end depolymerizes (30 min). This effect continues until the entire filament disappears (42 min). Apparently, other actin filaments in the immediate neighborhood were not affected by this process and independently continued their individual dynamics. Topographs exhibit a vertical height scale of 50 nm.

limiting the resolution of the AFM topography or causing imaging artifacts [14]. To visualize the actin polymerization in cytosol, we titrated the dilution of the cytosol to ensure a sufficient protein concentration for actin to polymerize and to prevent contamination of the scanning AFM tip by uncontrolled interaction with macromolecules resulting from the solution. At a total protein concentration of 0.8 mg/ml individual actin filaments were observed in the AFM topography

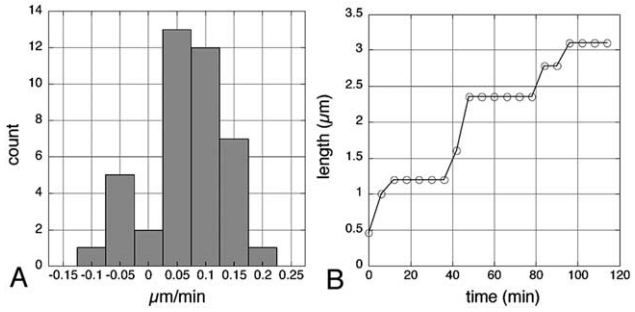


Fig. 2. Analyzing actin filaments in cell extract. A: Polymerization rate of all growing actin filaments. The average growth was $0.091 \pm 0.043$ μm/min and that of shrinking $-0.051 \pm 0.031$ μm/min. B: Polymerization of a single actin filament recorded over a time range of 115 min. The filament reversibly changes its state from growing (polymerizing) to being static.

(Fig. 1). Knowing that the contents of actin in HeLa cytosol is approximately 3% of the total protein [15], we estimated the concentration of actin in our assay to be around 0.6 μM. That the observed filaments were F-actin was confirmed by the finding that addition of cytochalasin D to the assay prevented the formation of the filaments (data not shown). It is important to mention that AFM provides three-dimensional data on the scanned object. Images presented in Fig. 1 also carry the information on the thickness ($z$-dimension) of the filaments. The $z$-data are color-coded: the lighter color corresponds to the thicker objects. Most of the filaments shown in Fig. 1 are of uniform color intensity and estimated to be 8–10 nm which fits well with the thickness of an individual actin filament.

Time-lapse AFM topographs (Fig. 1B) show individual actin filaments growing in a heterogeneous manner. While most of the filaments (85%, 279 filament ends scored) remained mainly unchanged in their length, others grew at variable rates. Occasionally, individual filaments disappeared indicating that they depolymerized. Fig. 2A shows the polymerization rates of various filaments observed over the time range of more than 5 h. Interestingly, most actin filaments interrupted their polymerization for a while and then continued to grow or to shrink again. According to the rates found it is possible to distinguish three classes to describe the polymerization process: an inactive phase with no or nearly no polymerization, a polymerization phase exhibiting an average rate of $0.091 \pm 0.043$ μm/min ($n = 36$; mean value ± S.D.) and a depolymerization phase showing a rate of $-0.051 \pm 0.031$ μm/min. Those values are close to the ones found by Fujiwara et al. at comparable concentrations with purified actin [4]. Fig. 2B shows the growth behavior of a single actin filament over the time range of 5 h. From this analysis, it becomes clear that the actin filaments exhibit the possibility to switch between the three growth phases of depolymerization, polymerization and inactivity (Fig. 2B and data not shown).

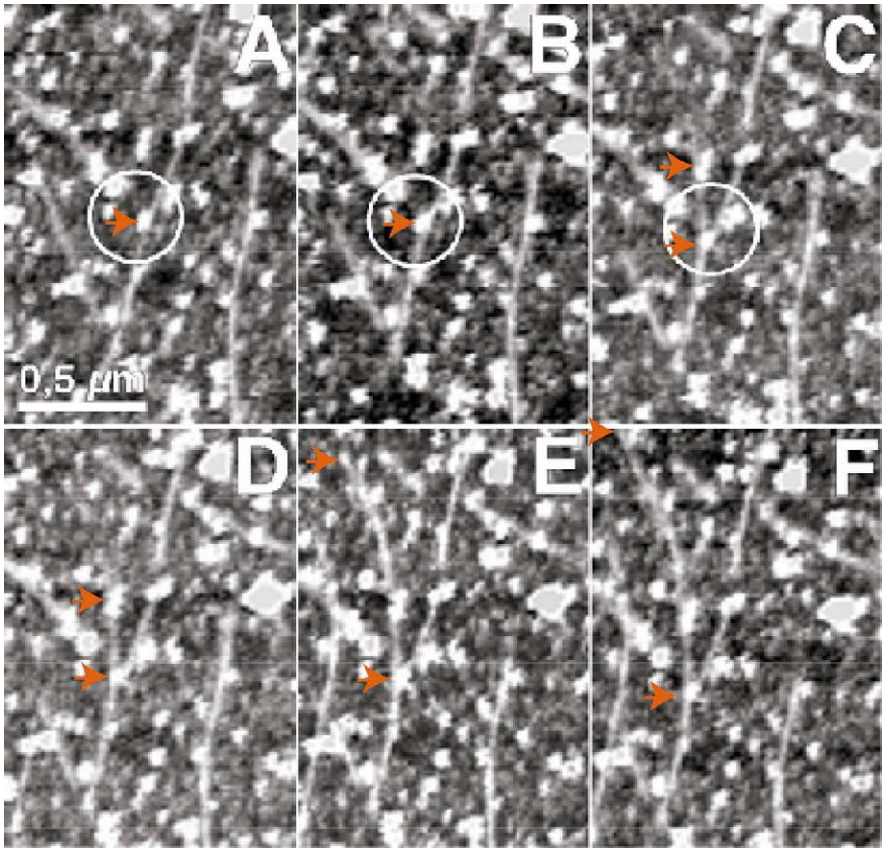


Fig. 3. Branching of an actin filament. A: Selected area of actin filaments. The white circle indicates a region of an actin filament being associated with an endosome. B: Same area imaged after a time course of 6 min. C,D: After 12 and 18 min, however, an actin filament grows from the endosomes labeling the actin filament. Apparently, the growing actin filament interacts with another endosome. After this, the actin filament continued its growth (E, $t = 24$ min and F, $t = 30$ min). Topographs exhibit a vertical height scale of 50 nm. Arrowheads indicate the ends of the filament.

### 3.2. Branching and junction of actin filaments

Some of the branching and cross-linking proteins such as the Arp2/3 complex are contained in endosomes [3,16,17]. Moreover, it was recently shown that membrane organelles and endosomes in particular can induce actin polymerization [16]. To study the behavior of the actin network in the presence of a defined membrane organelle population we included purified endosomes [11] in our assay.

From the actin networks, it is possible to extract the branched and crosslinked filaments (Fig. 2). Among these examples, branching angles varied between 40° and 90°, showing a broad distribution. Similar data were obtained by cryoelectron tomography ([18]). These observations are consistent with the presence of a variety of actin-cross-linking and actin-branching proteins that connect actin filaments to each other at variable angles. Although the filaments grew onto the mica surface without being exposed to any mechanical stress, some of the filaments were bent close to their site of attachment. This presumably was caused by some unidentified actin-binding proteins that link one end of a filament to the side of another one. In most cases, the branches and junctions of actin filaments were covered by vesicle-like structures (Fig. 3) which are assumed to present endosomes. These observations are consistent with the recent studies addressing the role of actin in the endocytic pathway [17]. Endosomes interacting with actin filaments can induce their branching, bending or mediate their interaction with the cell membrane [17].

We have shown that time-lapse AFM can be applied to study in vitro complex biological systems at high resolution. The AFM topographs revealed molecular insights into the formation of actin networks, growth, shrinkage, branching, junction, and into the interaction of actin with endosomes. Although the wealth of information potentially revealed by AFM may show important and novel insights into in vitro systems, technical improvements may soon allow more detailed insights. Technological developments will concentrate on the combination of high-resolution fluorescence microscopy and AFM. Individual constituents of the cell extract will be labeled with fluorescence markers to reveal insights into the mechanisms of actin and endosomal function. Improved time resolution of the AFM will be available by establishing fast-speed AFM currently enabling to record ~20 images per second.

*Acknowledgements:* We are grateful to Isabel Richter for technical assistance and to Tony Hyman and Laurence Pelletier for comments on the manuscript.

## References

[1] Schmidt, T., Schütz, G.J., Baumgartner, W., Gruber, H.J. and Schindler, H. (1996) Proc. Natl. Acad. Sci. USA 93, 2926–2929.
[2] Weiss, S. (1999) Science 283, 1676–1683.
[3] Pollard, T.D., Blanchoin, L. and Mullins, R.D. (2000) Annu. Rev. Biophys. Biomol. Struct. 29, 545–576.
[4] Fujiwara, I., Takahashi, S., Tadakuma, H., Funatsu, T. and Ishiwata, S. (2002) Nat. Cell Biol. 4, 666–673.
[5] Binnig, G., Quate, C.F. and Gerber, C. (1986) Phys. Rev. Lett. 56, 930–933.
[6] Müller, D.J. and Anderson, K. (2002) Trends Biotechnol. 20, S45–49.
[7] Drake, B. et al. (1989) Science 243, 1586–1588.
[8] Domke, J., Parak, W.J., George, M., Gaub, H.E. and Radmacher, M. (1999) Eur. Biophys. J. 28, 179–186.
[9] Engel, A. and Müller, D.J. (2000) Nat. Struct. Biol. 7, 715–718.
[10] Müller, D.J., Janovjak, H., Lehto, T., Kuerschner, L. and Anderson, K. (2002) Prog. Biophys. Mol. Biol. 79, 1–43.
[11] Gorvel, J.P., Chavrier, P., Zerial, M. and Gruenberg, J. (1991) Cell 64, 915–925.
[12] Möller, C., Allen, M., Elings, V., Engel, A. and Müller, D.J. (1999) Biophys. J. 77, 1050–1058.
[13] Amrein, M. and Müller, D.J. (1999) Nanobiology 4, 229–256.
[14] Schwarz, U.D., Haefke, H., Reimann, P. and Guntherodt, H.J. (1994) J. Microsc. 173, 183–197.
[15] Heacock, C.S., Eidsvoog, K.E. and Bamburg, J.R. (1984) Exp. Cell Res. 153, 402–412.
[16] Merrifield, C.J., Moss, S.E., Ballestrem, C., Imhof, B.A., Giese, G., Wunderlich, I. and Almers, W. (1999) Nat. Cell Biol. 1, 72–74.
[17] Qualmann, B., Kessels, M.M. and Kelly, R.B. (2000) J. Cell Biol. 150, F111–6.
[18] Medalia, O., Weber, I., Frangakis, A.S., Nicastro, D., Gerisch, G. and Baumeister, W. (2002) Science 298, 1209–1213.